

# **From Nano to Micro: Nanostructured Titania/PLGA Orthopedic Tissue Engineering Scaffolds Assembled by Three-dimensional Printing**

*Huinan Liu and Thomas J. Webster*

Division of Engineering, 182 Hope Street, Brown University, Providence, RI 02912, USA

## **Abstract**

A successful synthetic tissue engineering scaffold requires a hierarchical internal structure with interconnecting pores for nutrition transportation, cell infiltration and vascularization as well as nano-scale surface features favorable for cell attachment and long-term functions. However, traditionally, fabricating macro-scale scaffolds in a defined manner from nano-scale constituents has proved problematic. For example, the traditional porogen leaching techniques cannot precisely control the shape, size, location and interconnectivity of pores. In contrast, the use of three-dimensional (3D) printing, a rapid prototyping technique, can precisely produce pre-defined complex three-dimensional structures layer-by-layer based on patient medical information from computed tomography (CT) and/or magnetic resonance imaging (MRI). Previous in vitro studies demonstrated that two-dimensional PLGA (poly lactide-co-glycolide) scaffolds with well-dispersed titania nanoparticles enhanced osteoblast (bone-forming cell) adhesion and subsequent functions (such as calcium deposition). In this study, three-dimensional nanophase titania/PLGA scaffolds were fabricated via a novel 3D printing technique. Scanning electron microscopy (SEM) was used to characterize the structure and surface features of these 3D scaffolds. The SEM results demonstrated that the printed nano 3D scaffolds have a well-controlled, repeatable inner structure and, moreover, possessed uniformly dispersed titania nanoparticles which provided for nano-scale surface features throughout the PLGA matrix. The objective of the present in vitro study was to investigate osteoblast attachment and infiltration into such 3D composite scaffolds. Confocal microscopy was used to evaluate osteoblast attachment on the surface and infiltration into the porous structures. The results demonstrated that osteoblasts preferred the nano-scale roughness of the pore walls over that of the outer surface of the 3D nano scaffolds. Thus, this study suggests that these novel nano 3D scaffolds consisting of nanophase titania/PLGA composites created via the 3D printing technique may be promising for more effective orthopedic tissue engineering applications.

**Key words:** nanocomposite, tissue engineering scaffolds, titania, PLGA, 3D printing, orthopedic applications

## Introduction

The design of nanophase ceramic/polymer composites offers an exceptional approach to combine the advantages of biocompatible ceramics and biodegradable polymers to optimize physical, mechanical, and biological properties of tissue engineering scaffolds for bone regeneration because natural bone, similarly, is mainly composed of nanophase ceramic (such as hydroxyapatite crystals) and collagen nano-fibers. In this study, PLGA (poly-lactide-co-glycolide, also called poly-lactic-co-glycolic acid) was chosen as the model polymer since it is biodegradable, can be metabolized in the body and is approved by the U.S. Food and Drug Administration (FDA) for certain human clinical applications. Nanophase titania will be utilized as the model ceramic since it is readily formed at the surfaces of the current widely-used titanium implants and demonstrated excellent biocompatibility in previous studies [1-3]. Webster et al. have shown significant increases in osteoblast adhesion and subsequent long-term functions (such as collagen synthesis, alkaline phosphatase activity, and calcium-containing mineral deposition) on nanophase titania compacts compared to traditional micro-sized titania compacts [2-3]. Liu et al. demonstrated for the first time that the nanophase titania/PLGA composites with the closest surface roughness to natural bone at the nano-scale (provided by well-dispersed titania nanoparticles in PLGA) promoted bone cell adhesion and calcium deposition by osteoblasts the most [1]. However, to date, relative few advantages of nanocomposites have been incorporated into the orthopedic clinics due to the limited availability and flexibility of 3D fabrication techniques for nanocomposites.

Solvent-casting/porogen-leaching (SC/PL) techniques have been widely used to fabricate 3D porous polymer scaffolds for tissue engineering applications. Salt is the most commonly used porogen because it is easily available and very easy to handle. Briefly, this technique involves producing a suspension of polymers or ceramic/polymer composites in a solvent. Salt particles are ground and sieved into small particles and those of the desired size (most researchers use 100-200  $\mu\text{m}$  range particles) are transferred into a mold. A polymer or composite suspension is then cast into the salt-filled mold. The solvent is then removed by evaporation in air and/or in vacuum. After the evaporation of the solvent, the salt crystals are leached away by immersion in water to form a porous structure. In this technique, the pore size can be controlled by the size of the porogen particles and the porosity can be controlled by the amount of porogen added into the polymer or composite suspension. However, solvent-casting/porogen-leaching techniques have two main disadvantages. First, certain critical variables such as pore shape and inter-pore openings are still not well controlled in this technique. Second, if nanophase ceramic particles were used to make nanocomposite scaffolds in this technique, nanoparticles may interfere with the porogen leaching process, which will result in residual porogen particles in the final tissue engineering products, and thus, have adverse effects on their biocompatibility.

Another technique, called phase separation and emulsion freeze drying, has been developed based on the thermodynamic principle for the fabrication of 3D porous polymer scaffolds [4-5]. This technique involves liquid-liquid phase separation and solid-liquid phase separation. Liquid-liquid phase separation was mainly used for preparing polymer scaffolds. Solid-liquid phase separation, also called emulsion freeze drying, could be applied to both polymers and composites. Briefly, this technique could be achieved by lowering the temperature to induce solvent crystallization from a polymer or composite suspension (solid phase formation in a liquid phase). After the removal of the solvent crystals (sublimation or solvent exchange), the space originally taken by the solvent crystals becomes pores. For example, Liu et al. used this technique to prepared collagen/hydroxyapatite composite scaffolds [6]. Specifically, hydroxyapatite powder was added into a collagen solution, and homogenized by a speed stirrer. The mixture was then poured onto petri dishes, and rapidly transferred into a refrigerator at  $-30^{\circ}\text{C}$  to solidify the mixture and induce solid-liquid phase separation. The solidified mixture was maintained at that temperature for 2 hours, and then lyophilized for 2 days. The final collagen/hydroxyapatite scaffolds were porous with three-dimensional interconnected fiber microstructure and demonstrated an

uneven pore size from 50 to 150  $\mu\text{m}$ . Although this technique is advantageous as it does not require a porogen and an extra washing/leaching step, the phase diagrams of the polymer-solvent or composite-solvent systems must be fully characterized which would significantly increase the difficulties in controlling the process especially when composites are involved. Moreover, the pores formed using phase separation techniques usually have irregular shapes, have diameters on the order of a few to tens or hundreds of microns and are often not uniformly distributed.

One of the common shortcomings of these fabrication technologies discussed above is the lack of precise control of the three-dimensional internal and external architecture of the scaffolds, which is very disappointing since osteoblasts prefer well-ordered structures rather than random structures [7-10]. To tackle this problem, a novel aerosol based 3D printing technique developed by OPTOMECH<sup>®</sup> will be used for the first time to process nanophase ceramic/polymer scaffolds for bone tissue engineering applications because natural bone, similarly, builds its 3D nano-micro-macro hierarchical structures from its nanocomponents. The main advantage of this technique is its ability to rapidly produce complex-shaped tissue engineering scaffolds with well-controlled three-dimensional architecture and pore structures layer-by-layer from a pre-defined computer-aided design (CAD) model. Moreover, this technique allows us to directly produce bone substitutes with complex three-dimensional structures based on patient medical information from computed tomography (CT) and/or magnetic resonance imaging (MRI). The objective of this study was to test the effectiveness of this 3D printing technique for nanocomposite fabrication and the cytocompatibility (such as osteoblast (bone-forming cells) adhesion and infiltration onto these 3D printed nanocomposite scaffolds). In this current study, the structure and surface features of these 3D nanophase titania/PLGA scaffolds were characterized by scanning electron microscopy (SEM). Confocal laser scanning microscopy was used to evaluate osteoblast attachment on the surface and infiltration into the porous structures.

## Materials and Methods

### *Preparation of 3D Nanophase Titania/PLGA Scaffolds*

PLGA (poly-lactide-co-glycolide) pellets (50/50 wt.% poly(DL-lactide/glycolide); molecular weight: 100,000-120,000 g/mol; intrinsic viscosity: 66-80  $\text{cm}^3/\text{g}$ ; polydispersity: 1.8; density: 1.34  $\text{g}/\text{cm}^3$ ; glass transition temperature  $T_g$ : 45-50 $^\circ\text{C}$ ) were purchased from Polysciences, Inc. (Warrington, PA). Nanophase titania powder (Nanotek<sup>®</sup>) were purchased from Nanophase Technologies Corporation (Romeoville, IL). The purity of the titania powder was 99.5+%, the particle size was 32 nm which was calculated from BET adsorption measurements, the particle morphology was nearly spherical as shown in the TEM image (Figure 1), and the crystalline phase was 80% anatase/20% rutile [11]. Bulk and true density of this titania powder were 0.25  $\text{g}/\text{cm}^3$  and 3.96  $\text{g}/\text{cm}^3$ , respectively.

PLGA pellets were dissolved in chloroform (Mallinckrodt Technical) at 50 $^\circ\text{C}$  in a water bath for 40 minutes. Nanophase titania powder was then added to the PLGA solution to give a 30/70 ceramic/polymer weight ratio. The composite mixture was sonicated for 10 minutes using a S-250D Branson<sup>®</sup> Digital Sonifier (Branson, Inc., Danbury, CT) with its tip immersed in the mixture. This sonifier permits the application of ultrasonic energy to the suspensions on a pulsed basis. In this study, the intensity was set at 400 W and the pulse width was set as 60% of the duty cycle out of 1 second cycle time. This intermittent operation permits high intensity sonication while avoiding heat build-up in the processed suspensions.

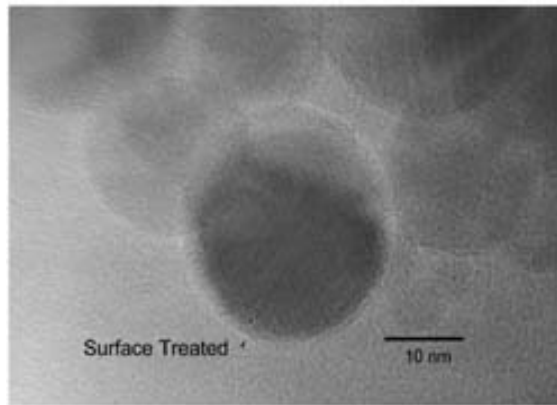
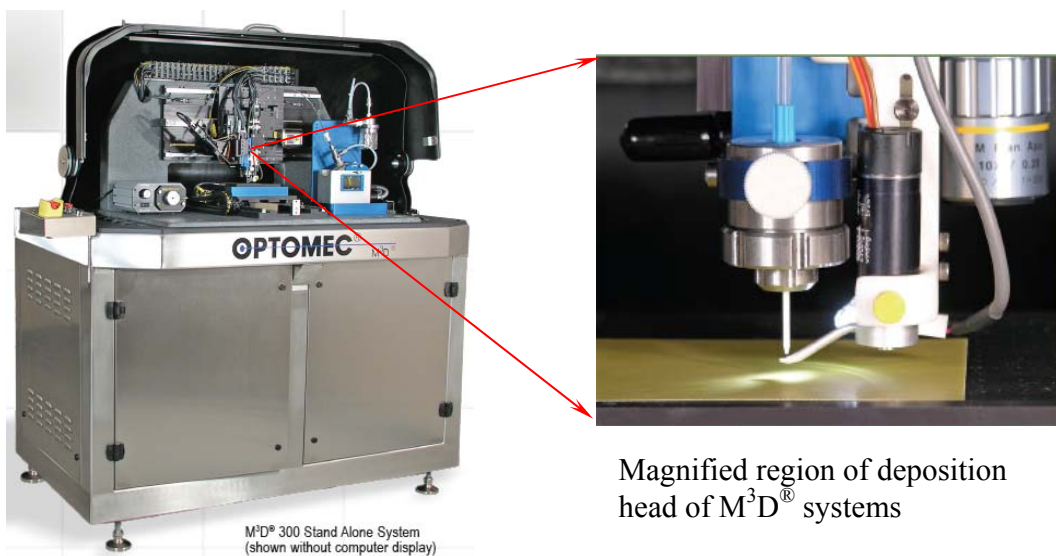
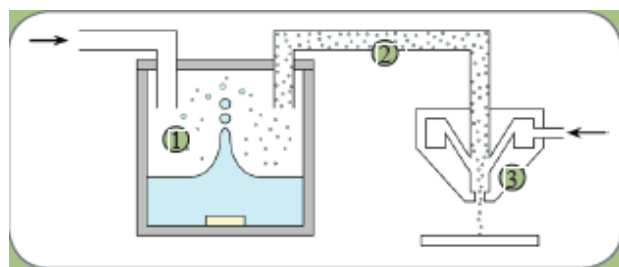


Figure 1: TEM image of nanophase titania powder. Magnification bar is 10 nm.



Magnified region of deposition head of M<sup>3</sup>D<sup>®</sup> systems

Figure 2: Illustration of M<sup>3</sup>D<sup>®</sup> system. Top left is appearance of M<sup>3</sup>D<sup>®</sup> system.. Top right is a closer look of deposition head. Bottom right is schematic principles of this aerosol based 3D printing technique. (Obtained from OPTOMECC<sup>®</sup>)



Schematic principles of aerosol based 3D printing

After sonication, the M<sup>3</sup>D<sup>®</sup> system developed by OPTOMECC<sup>®</sup> was used for 3D printing (Figure 2). First, the well dispersed composite suspension was fed into a reservoir in the M<sup>3</sup>D<sup>®</sup> system and then aerosolized in an atomizer to create a dense aerosol of tiny droplets; the aerosol was carried by a gas to the deposition head and focused by a second gas flow within the deposition head; and finally the resulting high velocity stream was “sprayed” onto the substrate layer by layer according to pre-designed

CAD (computer-aided design) models. Using this technique, bone fracture data acquired by computer-aided tomography (CT) can be transferred into CAD models and used to direct the fabrication of versatile bone substitutes.

The 3D printed nanocomposite scaffolds were dried in air at room temperature for 24 hours and dried in an air vacuum chamber at room temperature for 48 hours. The final composite scaffolds were 1 cm × 1 cm squares with a thickness of 0.3 mm. These scaffolds were sterilized by soaking in 70% ethanol for 30 minutes and were dried completely before performing experiments with cells.

### ***Characterization of 3D Nanophase Titania/PLGA Scaffolds***

Surface topographies and 3D structures of the 3D printed nanophase titania/PLGA composites were characterized according to standard scanning electron microscopy techniques using a LEO 1530 Field Emission Scanning Electron Microscope (FSEM) at a 5 kV accelerating voltage. Substrates were sputter-coated with a thin layer of gold-palladium using a Hummer I Sputter Coater (Technics) in a 100 millitorr vacuum argon environment for 3 minutes with 0.01 Amp of current. The areal analysis technique was used to quantitatively measure the pore size and porosity. SEM images taken at 60 kX magnifications were used to determine nanophase titania dispersion in PLGA.

### ***In Vitro Cytocompatibility Studies***

Human osteoblasts (bone-forming cells; CRL-11372 American Type Culture Collection) were cultured in Dulbecco's modified Eagle's medium (DMEM; GIBCO, Grand Island, NY) supplemented with 10% fetal bovine serum (FBS; Hyclone) and 1% penicillin/streptomycin (P/S; Hyclone) under standard cell culture conditions, that is, a sterile, 37°C, humidified, 5% CO<sub>2</sub>/95% air environment. Cells at passage numbers 5-6 were used in the experiments.

All sterilized scaffolds were placed in tissue culture plates (Corning, New York) and were rinsed three times with sterilized phosphate buffered saline (PBS; a solution containing 8 g NaCl, 0.2 g KCl, 1.5 g Na<sub>2</sub>HPO<sub>4</sub>, and 0.2 g KH<sub>2</sub>PO<sub>4</sub> in 1000 ml deionized water adjusted to a pH of 7.4; all chemicals from Sigma). Osteoblasts were seeded at a concentration of 2500 cells/cm<sup>2</sup> onto the substrates of interest in 2 ml DMEM supplemented with 10% FBS and 1% P/S and were then incubated under standard cell culture conditions for 4 hours. After that time period, non-adherent cells were removed by rinsing with PBS and adherent cells were then stained with DAPI nucleic acid stain (Invitrogen); the cell nuclei were thus visualized and counted under a confocal laser scanning microscope (Leica TCS SP2 AOBs spectral confocal microscope, excitation wavelength 358 nm and emission wavelength 461 nm). Two detection channels were used in this study: one was for imaging fluorescence from stained cells and another was for collecting bright field images of scaffolds. Leica's confocal software, LCS version 2.5, was used for 3D-scanning image acquisition and 3D reconstruction. Cell counts were expressed as the average number of cells adhered around the pores and adhered on the surfaces away from the pores determined in twenty fields of view. All experiments were run in triplicate.

### ***Osteoblast Morphologies***

Osteoblast morphologies on the composite scaffolds were observed using a JEOL JSM-840 Scanning Electron Microscope. For this purpose, after the 4 hour adhesion test, adherent osteoblasts on the substrates were fixed with 2 % glutaraldehyde (Electron Microscopy Sciences) in 0.1 M cacodylate (pH 7.4; Electron Microscopy Sciences) for 30 minutes at 4°C. After washing with cacodylate buffer, the cells were secondarily fixed with 1 % osmium tetroxide (Electron Microscopy Sciences) in 0.1 M cacodylate (pH 7.4) for 30 minutes at 4°C. The cells were dehydrated through a series of ethanol solutions (from 30, 50, 70, 90, to 100 %; AAPER) and were finally dried by critical point drying (CPD; LADD Research Industries). Specifically, the specimens were immersed in liquid CO<sub>2</sub> until there was a complete exchange of liquid CO<sub>2</sub> for the ethanol in the specimens. The specimens were then heated

above 34°C under 7.6 MPa where all liquid CO<sub>2</sub> was converted to gaseous CO<sub>2</sub> and the specimens were dry. Before imaging, all the specimens were sputter-coated with a thin layer of gold-palladium using a Hummer I Sputter Coater (Technics) in a 100 millitorr vacuum argon environment for 3 minutes with 0.01 Amp of current. Cell morphologies were imaged using a 5 kV accelerating voltage, and 3×10<sup>-11</sup> Amp probe current.

### ***Statistical Analysis***

Numerical data were analyzed using Student *t* test; statistical significance was considered at  $p < 0.05$ .

## **Results and Discussion**

### ***Characterization of 3D Nanophase Titania/PLGA Scaffolds***

The 3D printed nanophase titania/PLGA composite scaffolds had well-ordered 3D structures as designed (Figure 3). The pores had a cubic shape and pore sizes were controlled at 100 μm. The porosity was 32%. As mentioned, the pore size, shape and porosity can be precisely controlled by the pre-designed CAD model using this aerosol based 3D printing technique. The architecture of these 3D nanocomposite scaffolds was significantly different from that of formed from porogen leaching or phase separation techniques which produce randomly packed pores. Clearly, the uncontrolled, random pore structures cause a lack of predictable biological properties and mechanical properties. The advantage of this interconnected, ordered pore network created in this study is that it provides a regulated pathway of suitable dimensions for nutrient and waste transportation as well as vascularization throughout the scaffolds. Moreover, the surfaces of such nanocomposite scaffolds demonstrated uniform dispersion of titania nanoparticles after 3D printing (Figure 4). It was previously reported that well dispersed titania nanoparticles in PLGA promoted initial osteoblast adhesion and long-term functions such as calcium deposition [1].

### ***In Vitro Cytocompatibility Results***

The in vitro osteoblast adhesion results demonstrated that these 3D scaffolds further promoted osteoblast infiltration into porous structures compared to previous nanostructured surfaces. The SEM image in Figure 5 shows a well-spread osteoblast attached on the nanocomposite surface. The confocal image in Figure 6 shows enhanced osteoblast adhesion around pore structures of such 3D printed nanocomposite scaffolds. Quantitative results of cell counts demonstrated that osteoblast infiltration onto the pore structures was 4.2 times greater than osteoblast adhesion onto the scaffold surfaces, as shown in Figure 7. Increased osteoblast infiltration into 3D porous structures is a crucial prerequisite for enhancing subsequent new bone ingrowth.

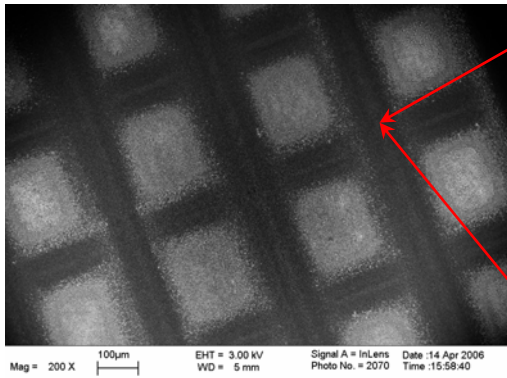


Figure 3: SEM micrograph of 3D nanocomposite scaffolds. Bar=100 µm.

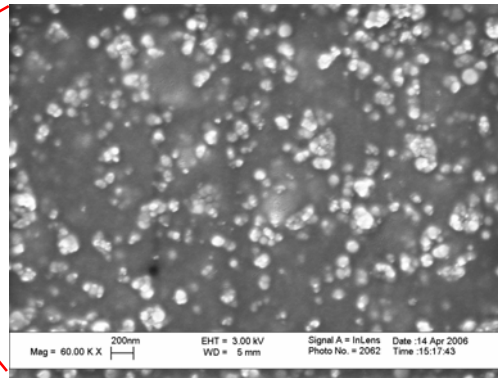


Figure 4: SEM micrograph of a magnified region of the 3D nanocomposite surface. Bar=200 nm.

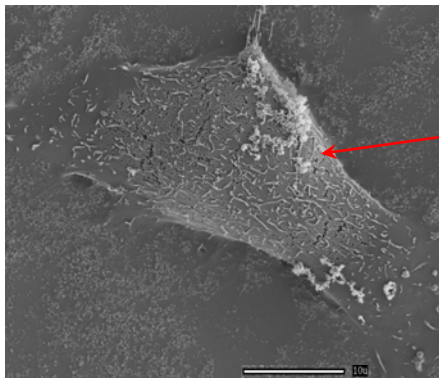


Figure 5: SEM micrograph of an osteoblast adhering on the nanocomposite surface. Bar=10 µm.

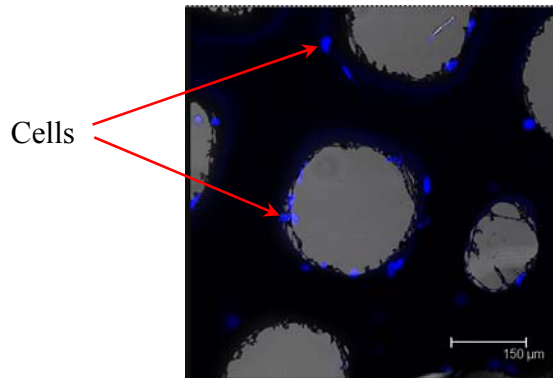


Figure 6: Confocal micrograph of osteoblasts adhering around pore structures of 3D nanocomposite scaffold. Bar=150 µm.

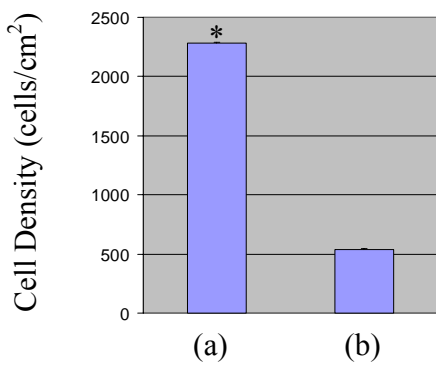


Figure 7: (a) the average number of osteoblasts adhered to pore structures. (b) the average number of osteoblasts adhered to the surfaces away from pores. Values are mean  $\pm$  SD; n = 3; \* $p < 0.05$  compared to (b).

## Conclusions

So far, results of this study have evaluated a promising new orthopedic nanocomposite and a means of fabricating a macro structure from such nanomaterials that can mimic properties of natural bone, thus, providing a new material and approach for more effective orthopedic applications.

Considering these exciting results, future work is needed to focus on understanding cell interactions with various nanostructured 3D patterns and determining the mechanisms for improved osteoblast functions and infiltration on these 3D nanocomposite scaffolds.

## Acknowledgements

The authors would like to thank the NSF for a Nanoscale Exploration Research (NER) grant and OPTOMECH<sup>®</sup> for the assistance with the M<sup>3</sup>D<sup>®</sup> printing system.

## References

- [1] Liu, H., Slamovich, E.B., and Webster, T. J., Increased osteoblast functions among nanophase titania/poly(lactide-co-glycolide) composites of the highest nanometer surface roughness. *Journal of Biomedical Materials Research*, 78A(4), pp. 798-807, 2006.
- [2] Webster, T.J., Siegel, R.W., and Bizios, R., Osteoblast adhesion on nanophase ceramics. *Biomaterials*, 20(13), pp. 1221-1227, 1999.
- [3] Webster, T.J., Ergun, C., Doremus, R.H., and Siegel, R.W., Enhanced functions of osteoblasts on nanophase ceramics. *Biomaterials*, 21(17), pp. 1803-1810, 2000.
- [4] Whang, K., Thomas, C. H., Healy, K. E., and Nuber, G., Novel method to fabricate bioabsorbable scaffolds. *Polymer*, 36(4), pp. 837-842, 1995.
- [5] Nam, Y.S., and Park, T.G., Porous biodegradable polymeric scaffolds prepared by thermally induced phase separation. *Journal of Biomedical Materials Research*, 47(1), pp. 8-17, 1996.
- [6] Liu, L., Zhang, L., Ren, B., Wang, F., and Zhang Q., Preparation and characterization of collagen-hydroxyapatite composite used for bone tissue engineering scaffold. *Artificial Cells, Blood Substitutes, and Biotechnology*, 31(4), pp. 435-448, 2003.
- [7] Badami, A.S., Kreke, M.R., Thompson, M.S., Riffle, J.S., and Goldstein, A.S., Effect of fiber diameter on spreading, proliferation, and differentiation of osteoblastic cells on electrospun poly(lactic acid) substrates. *Biomaterials*, 27(4), pp. 596-606. 2006.
- [8] Matsuzaka, K., Walboomers, X.F., de Ruijter, J.E., and Jansen, J.A., The effect of poly-L-lactic acid with parallel surface micro groove on osteoblast-like cells in vitro. *Biomaterials*, 20(14), pp. 1293-1301, 1999.
- [9] Chehroudi, B., McDonnell, D., and Brunette, D.M., Effects of micromachined surfaces on formation of bonelike tissue on subcutaneous implants as assessed by radiography and computer image processing. *Journal of Biomedical Materials Research*, 34(3), pp. 279-290, 1997.
- [10] Wieland, M., Textor, M., Chehroudi, B., and Brunette, D.M., Synergistic interaction of topographic features in the production of bone-like nodules on Ti surfaces by rat osteoblasts. *Biomaterials*, 26(10), pp. 1119-1130, 2005.
- [11] <http://www.nanophase.com/catalog/>